

# Analysis of Rock Damage Characteristics Based on Particle Discrete Element Model

Zhen-long Zhao · Xiao Wang · Zhi-jie Wen

Received: 29 August 2016 / Accepted: 4 September 2017 / Published online: 8 September 2017  
© Springer International Publishing AG 2017

**Abstract** Rock is a heterogeneous medium that is composed of minerals of various sizes. Under the action of external loads, the generation, propagation and coalescence of microdefects in the rock mass determines the macroscopic deformation and fracture of rock. To understand the damage law of rock and to reveal the evolution of dynamic failure, a uniaxial compression model was established based on particle flow code. Acoustic emission and energy characteristics of rock damage were analyzed, and the damage constitutive models of rock were discussed. During rock uniaxial compression, acoustic-emission events undergo a relatively quiet, sudden increase and sharp decrease for three periods, which corresponds to the compaction and elastic deformation stage, yield stage and post-peak stage in the stress–strain curve. Before

the yield stress is reached, the proportion of bond and strain energies is larger. Friction energy accounts for a small proportion of the total energy, and a reciprocal relationship exists between them. The constitutive model that is based on friction energy can better reflect the variation in stress and strain, then the constitutive model based on acoustic-emission parameters.

**Keywords** Rock mass · Damage evolution · Acoustic emission · Energy · Constitutive model · Particle flow code

## 1 Introduction

Rock is a porous medium that is composed of minerals of various sizes that are bonded together by cements (Abdollahipour and Marji 2017; Hu et al. 2017). Many small cracks exist inside rock. Under the effect of an external load, preexisting fissures in the rock evolve, and new cracks emerge and develop. The initiation, propagation and linking of these tiny cracks at a microscale results in rock macrofailure (Tan et al. 2013; Zhou et al. 2014; Zhao et al. 2016; Lee et al. 2017; Bahrani and Kaiser 2017; Wang and Cao 2017). During rock deformation and fracture, an acoustic emission (AE) phenomenon occurs and internal energy undergoes a complex transformation, which can help people understand the laws of rock deformation and

---

Z. Zhao · X. Wang · Z. Wen (✉)  
State Key Laboratory of Mining Disaster Prevention and Control Co-founded by Shandong Province and the Ministry of Science and Technology, Shandong University of Science and Technology, Qingdao 266590, People's Republic of China  
e-mail: zl\_zhao\_cn@163.com

X. Wang  
e-mail: wangchxizo@163.com

Z. Wen  
e-mail: skziwen@163.com

X. Wang  
School of Civil Engineering, Southeast University, Nanjing 210096, People's Republic of China

failure, the evolution of rock-dynamic failures and solve the rock-mass-engineering stability.

Scholars have studied the AE characteristics of rock during compression. Khazaei et al. (2015) conducted 73 uniaxial tests on specimens of shale, limestone and dolostone rocks, and monitored acoustic emission during the tests to study the evolution of the b-value, maximum released energy, total released AE energy and total consumed energy in different rocks. Filipussi et al. (2015) studied the mechanical behavior of Argentinian rock and analyzed the damage level and failure types of the rock through the AE parameters. Moradian et al. (2014) carried out uniaxial compression tests of granite specimens that contain pre-existing flaws to understand the fracture process in brittle rocks by analyzing the relationship of the AE signal, the failure mode and the specimen stress–strain curve. Liang et al. (2017) carried out three kinds of confining pressure loading–unloading tests during the residual stage of argillaceous limestone specimens, and studied the mechanical properties of rock in the residual phase by analyzing the variation in stress, strain and AE.

Rock deformation and failure can be regarded as a process of energy dissipation. Therefore, many scholars have studied the damage law of rock from the point of view of energy dissipation. Zhao and Xie (2008) used the energy method to study rock failure, and included the transformation and calculation principle between elastic energy, plastic property, surface energy, radiation energy and kinetic energy, and their effects on rock failure. Liu et al. (2016) established a new damage constitutive model based on energy dissipation to describe the behavior of rocks under cyclic loading. Hu et al. (2016) analyzed the failure of deep-sea cobalt-rich crust specimens systematically from the point of view of elasticity, dissipation energy and total energy through uniaxial loading and unloading tests. Bańka et al. (2017) applied the regression-analysis method to study the relationship between calculated energy changes that occur in tremor-prone rock layers and typical runs of induced seismicity, and provided an example of the prediction of induced seismicity in a hard-coal mine.

The above studies have achieved outcomes, but few reports exist on the combination of damage and energy conversion in rock. Based on the theory of particle flow, a bonded-particle model (BPM) for rock was established by using particle flow code (PFC). The

damage characteristics and energy conversion of the PFC model during compression were monitored in real time by using FISH language, and the damage characteristics and constitutive model of rock are discussed based on this approach.

## 2 Model Generation and Calibration

### 2.1 PFC Fundamental

PFC was developed based on discrete-element theory (Cundall and Strack 1979), which has good applicability to analyze the damage evolution mechanism and failure of rock at the microscale. PFC uses explicit time-step cyclic operation rules to calculate particles of a model. The constitutive relationship between particles is the relationship between the force and the displacement, and the motion equation is that of Newton's second law (Ning et al. 2015; Meng 2017; Jin et al. 2017).

Particles can be bound together at contacts. Two types of bonds exist between particles, and these include the contact bond and the parallel bond (Tan et al. 2016; Lv et al. 2017; Wen et al. 2017). Contact-bond glue is of a small size that acts only at the contact point, whereas parallel-bond glue is of a finite size that acts over either a circular or a rectangular cross-section between the particles. The contact bond can only transmit a force, which is suitable for simulating granular materials (e.g., soil mass). The parallel bond can transmit a force and a moment, which is suitable for simulating dense materials such as rock. A parallel bond can be envisioned as a set of elastic springs that are distributed uniformly over a rectangular cross-section that lies on the contact plane and is centered at the contact point (Khazaei et al. 2016; Mehranpour and Kulatilake 2017), as shown in Fig. 1.

The maximum normal and shear stresses ( $\bar{\sigma}$  and  $\bar{\tau}$ , respectively) that are carried by the bonding material can be written as:

$$\begin{cases} \bar{\sigma} = \frac{T}{A} + \frac{|M|\bar{R}}{I} \\ \bar{\tau} = \frac{|V|}{A} + \frac{|M_r|\bar{R}}{J} \end{cases} \quad (1)$$

where  $A$  and  $I$  are the area and moment of inertia, respectively, of the parallel-bond cross-section [given by Eq. (2)], and a positive  $T$  indicates the tension.

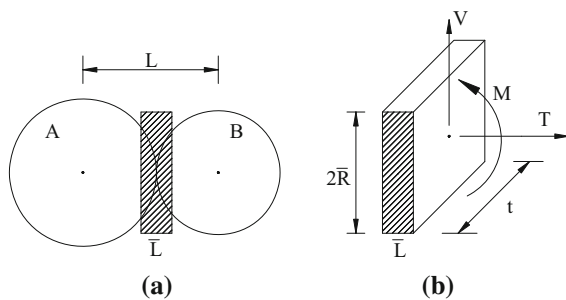


**Fig. 1** Diagram of two-dimensional parallel bond between particles: parallel-bond idealization (a), and forces carried in the bond material (b)

The beam cross-sectional area and moment of inertia can be expressed as:

$$\begin{cases} \bar{R} = \min(R^{[A]}, R^{[B]}) \\ A = 2\bar{R}t \\ I = \frac{1}{12}t(2\bar{R})^3 \end{cases} \quad (2)$$

## 2.2 Model Generation and Calibration

The bonded-particle model (Potyondy and Cundall 2004) for rock is generated by using parallel bonding. The particle-flow theory uses mesomechanical parameters to characterize the macroscopic physical properties of rock, and these parameters are not related directly to the macroscopic parameters of rock. Therefore, it is necessary to check and revise the microscopic parameters that are required by the model before the numerical simulation. While checking model parameters, a large number of numerical tests must be carried out. The “trial-and-error” method is used to debug the microparameters repeatedly, and the numerical results are compared with those in the laboratory or in an in situ test, so that the parameters meet the macromechanical rock response (Cheng et al. 2016; Chen 2017).

Based on the above analysis, a two-dimensional uniaxial compression model of 50 mm × 100 mm standard size was established. Table 1 shows that the macromechanical parameters of the model are close to those of the mechanical parameters of the granite specimens in laboratory tests. The micromechanical physical and mechanical parameters of the model are given in Table 2.

As shown in Figs. 2 and 3, the stress–strain curves and failure modes of the numerical model and granite specimen of an underground oil reserve of Qingdao in China are similar.

## 3 Evolution and Energy-Dissipation Law of Rock Damage

### 3.1 Acoustic Emission Characteristics of Rock Damage Process

Interparticle bonds will fracture under force when the interparticle bond strength is smaller than the strength that is transmitted between particles, which corresponds to microcracks in the rock (Ji and Di 2013; Hazzard et al. 2000). During microcrack propagation, damage energy will be released rapidly by elastic waves, and this phenomenon is termed AE (Sun et al. 2017; Shiotani et al. 2001). The AE characteristics of rock damage evolution can be analyzed by the number of broken bonds that are recorded in FISH language.

As shown in Fig. 4, the model begins to produce microcracks at point b (37.6% of the peak strength), and the first AE signal is emitted. From point b to stress yield point c (86.8% of the peak strength), the number of AE events is relatively low and there is an increase in the hit strength with the crack opening and expansion, which implies that the model enters the stable stage of crack propagation from the elastic stage.

With a further increase in load, the model enters the destabilization stage with a volume expansion and a deformation increase, and the stress–strain curve is a concave. In this stage, a large number of new cracks were produced, in addition to the further expansion of previous cracks. The convergence and coalescence of these cracks lead to the formation of macroscopic cracks (Fig. 4, point d), the interaction between cracks intensifies and the AE events increase rapidly.

After peak point d, the model shows characteristics of brittle failure along with a rapid decrease in axial stress. The number of cracks increases significantly and a maximum AE event of 30 is achieved. With a decrease in axial stress, the AE event decreases gradually. The AE event disappears as the model loses its bearing capacity. In this stage, the failure of the model is caused mainly by friction sliding along

**Table 1** Comparison of macromechanical parameters of granite specimens and PFC model

Data types	Young modulus (GPa)	Poisson ratio	Uniaxial compressive strength (MPa)
Simulation values	27.39	0.2300	129.0
Test values	26.88	0.2285	128.4
Errors (%)	1.9	0.7	0.5

**Table 2** Microscopic mechanical parameters of PFC model

Parameters	Minimum particle size (mm)	Particle size ratio	Normal stiffness (GPa)	Density (kg/m <sup>3</sup> )	Coefficient of friction	Parallel bond Normal stiffness (MPa)	Deformation of parallel bond Modulus (GPa)	Contact modulus of the particle (GPa)	Parallel bond Tangential stiffness (MPa)
Values	0.3	1.66	3.0	2800	0.8	88 ± 10	43.0	5.0	160 ± 10

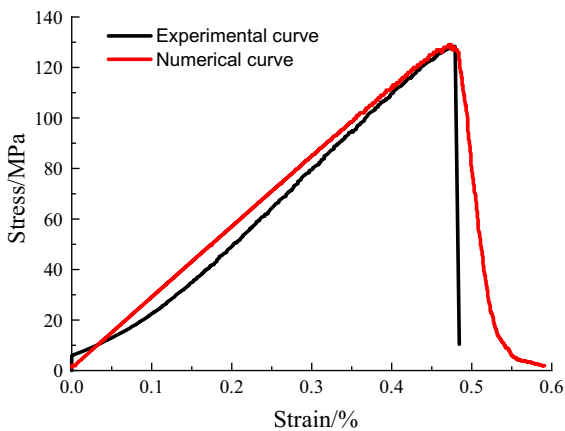


**Fig. 2** The stress–strain curves of granite specimen and PFC model

the macrocracks, which eventually results in model instability and failure.

### 3.2 Energy Characteristics of Rock Damage

As shown in Fig. 5, the sum of the friction energy (total energy dissipated by frictional sliding at all contacts), kinetic energy (total kinetic energy of all particles), strain energy (total strain energy of the entire assembly stored at all contacts) and bond energy

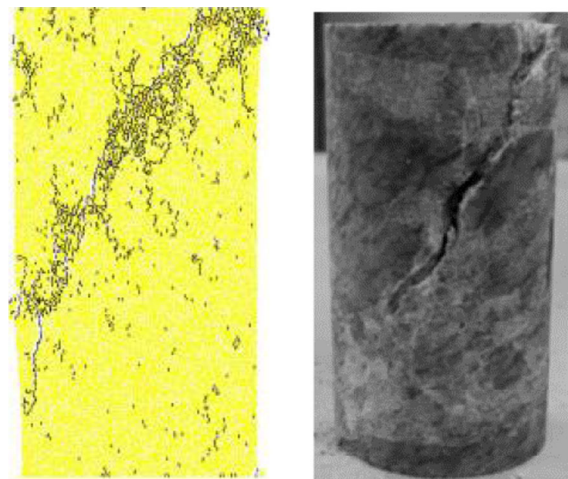


**Fig. 3** The failure modes of granite specimen and PFC model

(total strain energy of the assembly stored in parallel bonds) is almost equal to the boundary energy (total accumulated work done by walls on the assembly) before the yield stress point *c*. The proportion of bond energy and strain energy is larger, and this part of the energy is associated with crack generation and expansion. Its growth and decline are related to material damage. In contrast, the friction energy (on behalf of the effect of the crack) is very small because that crack generation must overcome the bond energy;

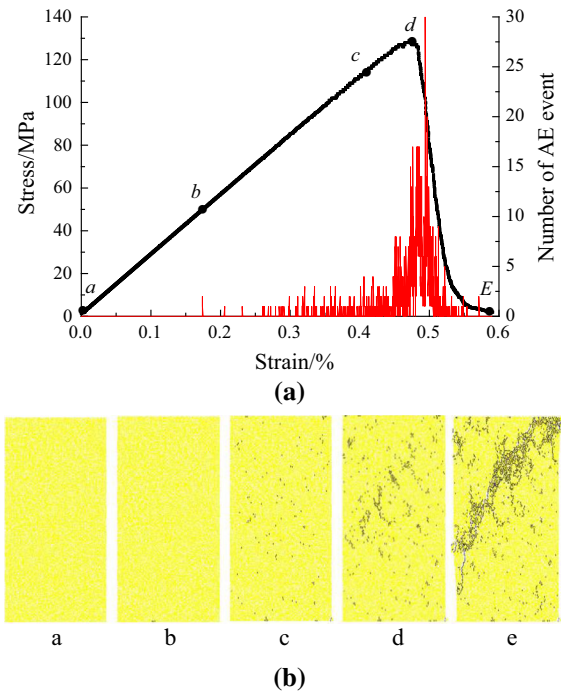


**Fig. 4** AE event and damage evolution of PFC model. **a** AE event of model, **b** damage evolution of model

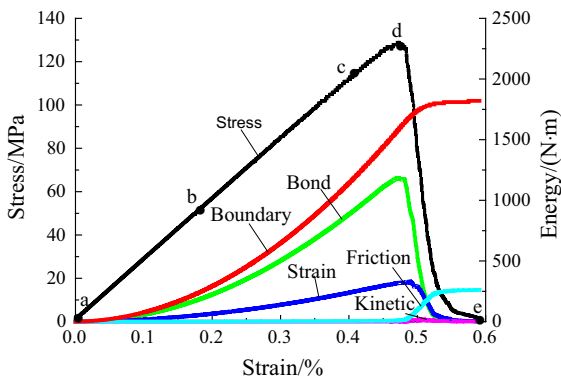


**Fig. 5** Energy evolution curves of PFC model

the cracks expand under the drive of strain energy, and friction begins to work after crack generation. After peak point *d*, the bonding energy and strain energy decrease sharply and the friction increases rapidly. The proportion of friction energy with further crack propagation increases gradually, thus friction is the main provider of residual rock strength. The proportion of kinetic energy is not large during the process, which is related to an internal dynamic balance of the

model. This result shows that the model deformation is not very violent and crack propagation is stable.

### 4 Establishment of Constitutive Model for Rock Damage

#### 4.1 Damage Variable

The concept of damage was first proposed by Kachanov (1958), who proposed that the continuous-damage factor and effective stress were used to describe the deterioration of metallic materials during creep fracture. Later, scholars (Unteregger et al. 2015; Zhu and Arson 2015; Wang et al. 2016; Ning et al. 2016; Liu et al. 2017; Xiao et al. 2017; Bahrani and Kaiser 2017) defined a variety of damage variables from different perspectives.

Because material damage is caused by changes in macroscopic physical properties and microstructures, we can choose the damage variable from the macro- and microaspects. In terms of the microscopic aspects, the crack number, length, area and volume can be selected. Macroscopically, the elastic coefficient, yield stress, elongation, density, AE and energy can be selected.

Because the AE, boundary energy and friction-energy curves have a similar variation law, the damage variable was defined by the AE, boundary energy and frictional energy.

#### 4.2 Constitutive Model of Rock Damage

According to Kachanov’s definition:

$$D = \frac{A_d}{A} \tag{3}$$

where *D* is the damage variable that represents cumulative damage, *A<sub>d</sub>* is the cross-sectional area of material damage in a certain period and *A* is the cross-sectional material area without damage initially.

Suppose that when the rock specimen loses its bearing capacity completely, the number of total cumulative acoustic emission events is *S*. The number per unit area damage is *S<sub>w</sub>*:

$$S_w = \frac{S}{A} \tag{4}$$

where  $S$  is the number of total cumulative acoustic emission events at the last moment and  $A$  is the cross-sectional area of the rock specimen without damage at the initial moment.

When the damage area reaches  $A_d$  at a certain moment, the cumulative amount of AE events is  $S_d$ :

$$S_d = S_w A_d = \frac{S}{A} A_d \tag{5}$$

where  $A_d$  is the cumulative damage area from the initial time to a certain moment.

Consider Eqs. (1) and (3) together, that

$$D = \frac{S_d}{S} \tag{6}$$

where  $D$  is the cumulative damage from the initial time to a certain moment.

Thus, based on acoustic emission parameters and the strain-equivalent principle (Lemaitre et al. 1999), constitutive model of rock damage under uniaxial compression is defined as:

$$\sigma = E\varepsilon(1 - D) = E\varepsilon\left(1 - \frac{S_d}{S}\right) \tag{7}$$

where  $\sigma$  is the axial stress of the rock specimen,  $E$  is the Young’s modulus and  $\varepsilon$  is the axial strain.

Similarly, the damage variables that are based on the boundary energy and frictional energy can be defined as well.

$$D_b = \frac{B_d}{B} \tag{8}$$

where  $D_b$  is the damage variable that is based on the boundary energy,  $B_d$  is the cumulative boundary energy when the damage area of the rock specimen reaches  $A_d$  and  $B$  is the total boundary energy when the rock specimen loses its bearing capacity completely.

$$D_f = \frac{F_d}{F} \tag{9}$$

where  $D_f$  is the damage variable that is based on the frictional energy,  $F_d$  is the cumulative frictional energy when the damage area of the rock specimen reaches  $A_d$  and  $F$  is the total frictional energy when the rock specimen loses its bearing capacity completely.

Equations (8) and (9) can be used to derive, the constitutive models of rock damage under uniaxial compression based on the boundary energy and friction energy are as follows:

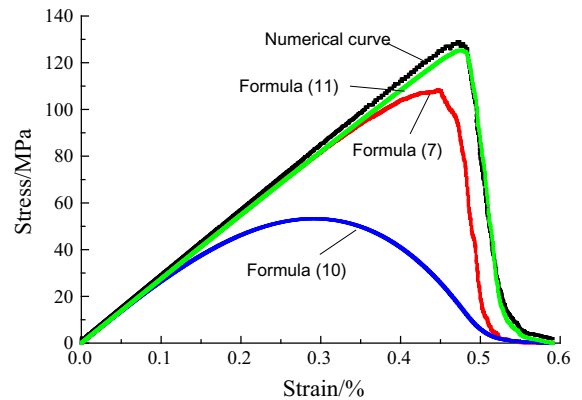


**Fig. 6** Fitted stress–strain curves

$$\sigma = E\varepsilon(1 - D_b) = E\varepsilon\left(1 - \frac{B_d}{B}\right) \tag{10}$$

$$\sigma = E\varepsilon(1 - D_f) = E\varepsilon\left(1 - \frac{F_d}{F}\right) \tag{11}$$

Figure 6 shows the stress–strain curves of rock that are fitted by Eqs. (7), (10) and (11) based on acoustic emission, boundary energy and friction energy parameters.

Figure 6 shows that the constitutive model that is based on friction energy is similar to the stress–strain curve of rock and can better reflect the variation in stress and strain, then the constitutive model based on boundary energy differs significantly from the stress–strain curve of rock. This occurs because the boundary energy needs to provide greater energy for rock damage from the start, whereas the boundary energy is absorbed by rock deformation and does not cause rock damage.

Because it is difficult to record the friction energy of real rock specimens during compression, AE parameters can be used to study the rock damage characteristics.

### 5 Conclusions

1. During uniaxial compression, the change in AE events can be divided into three stages. During the compression and elastic period, fewer AE events occur. During the failure stage, the number

increases suddenly. During the post-peak residual stage, the number decreases sharply.

2. Before the stress reaches the yield stress, the proportion of bond energy is larger, and this part of the energy is related to the formation and driving of cracks. In contrast, friction energy is the main provider of residual strength and accounts for a small proportion of the energy. A reciprocal relationship exists between them.
3. The constitutive model that is based on friction energy can better reflect the variation characteristics of stress and strain, and the constitutive model is based on the AE parameter. If it is difficult to record the friction energy of real rock specimens during the compression process, AE parameters can be used to study the rock-damage characteristics.

**Acknowledgements** The authors would like to acknowledge the support of Innovation Fund of Science and Technology of Post-graduate of College of Mining and Safety Engineering, Shandong University of Science and Technology (No. KYKC17006); the National Natural Science Foundation of China (Nos. 51304126, 51304235); the Fok Ying Tung Education Foundation (No. 141046); the China Postdoctoral Science Foundation (No. 2013M541918); the State Key Laboratory of Open Funds (No. SKLGDUEK1520); the Shandong Province Natural Science Foundation (Nos. ZR2017PEE018, ZR2016EEB23); the State Key research Development Program of China (No. 2016YFC0600708-3). In addition, we also thank Liwen Bianji for editing the English text of a draft of this manuscript.

## References

- Abdollahipour A, Marji MF (2017) Analyses of inclined cracks neighboring two iso-path cracks in rock-like specimens under compression. *Geotech Geol Eng* 35(1):169–181
- Bahrani N, Kaiser PK (2017) Estimation of confined peak strength of crack-damaged rocks. *Rock Mech Rock Eng* 50:1–18
- Bańka P, Chmiela A, Fernández MM, Muñizc ZF, Sanchezb AB (2017) Predicting changes in induced seismicity on the basis of estimated rock mass energy states. *Int J Rock Mech Min Sci* 95:79–86
- Chen PY (2017) Effects of microparameters on macroparameters of flat-jointed bonded-particle materials and suggestions on trial-and-error method. *Geotech Geol Eng* 35(2):663–677
- Cheng C, Chen X, Zhang SF (2016) Multi-peak deformation behavior of jointed rock mass under uniaxial compression: insight from particle flow modeling. *Eng Geol* 213:25–45
- Cundall PA, Strack OD (1979) A discrete numerical model for granular assemblies. *Geotechnique* 29(1):47–65
- Filipussi DA, Guzmán CA, Xargay HD, Hucailuka C, Torres DN (2015) Study of acoustic emission in a compression test of andesite rock. *Procedia Mater Sci* 9:292–297
- Hazzard JF, Young RP, Maxwell SC (2000) Micromechanical modeling of cracking and failure in brittle rocks. *J Geophys Res Atmos* 105(B7):16683–16697
- Hu JH, Liu SJ, Zhang RQ, Hu Q (2016) Energy analysis and experiment of breaking cobalt-rich crust. *Geotech Geol Eng* 34(4):1029–1035
- Hu SC, Tan YL, Zhou H, Guo WY, Hu DW, Meng FZ, Liu ZG (2017) Impact of bedding planes on mechanical properties of sandstone. *Rock Mech Rock Eng* 97:1–9
- Ji S, Di S (2013) Discrete element modeling of acoustic emission in rock fracture. *Theor Appl Mech Lett* 3(2):46–50
- Jin J, Cao P, Chen Y, Pu CZ, Mao DW, Fan X (2017) Influence of single flaw on the failure process and energy mechanics of rock-like material. *Comput Geotech* 86:150–162
- Kachanov LM (1958) Time of the rupture process under creep conditions. *Izy Akad Nank SSR Otd Tech Nauk* 12(8):26–31
- Khazaei C, Hazzard J, Chalaturnyk R (2015) Damage quantification of intact rocks using acoustic emission energies recorded during uniaxial compression test and discrete element modeling. *Comput Geotech* 67:94–102
- Khazaei C, Hazzard J, Chalaturnyk R (2016) A discrete element model to link the microseismic energies recorded in caprock to geomechanics. *Acta Geotech* 11:1351–1367
- Lee J, Hong JW, Jung JW (2017) The mechanism of fracture coalescence in pre-cracked rock-type material with three flaws. *Eng Geol* 223:31–47
- Lemaitre J, Sermage JP, Desmorat RA (1999) Two scale damage concept applied to fatigue. *Int J Fract* 97(1–4):67–81
- Liang Y, Li Q, Gu Y, Zou QL (2017) Mechanical and acoustic emission characteristics of rock: effect of loading and unloading confining pressure at the postpeak stage. *J Nat Gas Sci Eng* 44:54–64
- Liu XS, Ning JG, Tan YL, Gu QH (2016) Damage constitutive model based on energy dissipation for intact rock subjected to cyclic loading. *Int J Rock Mech Min Sci* 85:27–32
- Liu HZ, Xie HQ, He JD, Xiao ML, Zhuo L (2017) Nonlinear creep damage constitutive model for soft rocks. *Mech Time Depend Mater* 21(1):1–24
- Lv YX, Li HB, Zhu XH, Tang LP (2017) Bonded-cluster simulation of rock-cutting using PFC2D. *Clust Comput* 20(2):1289–1301
- Mehranpour MH, Kulatilake PHSW (2017) Improvements for the smooth joint contact model of the particle flow code and its applications. *Comput Geotech* 87:163–177
- Meng YW (2017) PFC2D simulation on stability of loose deposits slope in highway cutting excavation. *Geotech Geol Eng* 35(2):897–902
- Moradian Z, Einstein HH, Ballivy G (2014) Detection of cracking levels in brittle rocks by parametric analysis of the acoustic emission signals. *Rock Mech Rock Eng* 49:1–16
- Ning JG, Liu XS, Tan YL, Wang J, Tian CL (2015) Relationship of box counting of fractured rock mass with Hoek–Brown parameters using particle flow simulation. *Geomech Eng* 9(5):619–629
- Ning JG, Wang J, Tan YL, Shi XS (2016) Dissipation of impact stress waves within the artificial blasting damage zone in

- the surrounding rocks of deep roadway. *Shock Vib* 2016:1–13
- Potyondy DO, Cundall PA (2004) A bonded-particle model for rock. *Int J Rock Mech Min Sci* 41(8):1329–1364
- Shiotani T, Ohtsu M, Ikeda K (2001) Detection and evaluation of AE waves due to rock deformation. *Constr Build Mater* 15(5–6):235–246
- Sun XM, Xu HC, He MC, Zhang F (2017) Experimental investigation of the occurrence of rockburst in a rock specimen through infrared thermography and acoustic emission. *Int J Rock Mech Min Sci* 93:250–259
- Tan YL, Yin YC, Zhao TB (2013) Investigation of rock failure pattern in creep by digital speckle correlation method. *Adv Mater Sci Eng* 1:162–167
- Tan YL, Guo WY, Gu QH, Zhao TB, Yu FH, Hu SC, Yin YC (2016) Research on the rockburst tendency and AE characteristics of inhomogeneous coal–rock combination Bodies. *Shock Vib* 2:1–11
- Unteregger D, Fuchs B, Hofstetter G (2015) A damage plasticity model for different types of intact rock. *Int J Rock Mech Min Sci* 80:402–411
- Wang M, Cao P (2017) Experimental study of crack growth in rock-like materials containing multiple parallel pre-existing flaws under biaxial compression. *Geotech Geol Eng* 35(3):1023–1034
- Wang X, Wen ZJ, Jiang YJ (2016) Time–space effect of stress field and damage evolution law of compressed coal–rock. *Geotech Geol Eng* 34(6):1933–1940
- Wen ZJ, Wang X, Chen LJ, Lin G, Zhang HL (2017) Size effect on acoustic emission characteristics of coal–rock damage evolution. *Adv Mater Sci Eng*. doi:[10.1155/2017/3472485](https://doi.org/10.1155/2017/3472485)
- Xiao JQ, Ding DX, Jiang FL, Xu G (2017) Fatigue damage variable and evolution of rock subjected to cyclic loading. *Int J Rock Mech Min Sci* 47(3):461–468
- Zhao ZH, Xie HP (2008) Energy transfer and energy dissipation in rock deformation and fracture. *J Sichuan Univ (Engineering Science Edition)* 40(2):26–31
- Zhao ZH, Lv XZ, Wang WM, Tan YL (2016) Damage evolution of bi-body model composed of weakly cemented soft rock and coal considering different interface effect. *Springerplus* 5(1):292
- Zhou XP, Cheng H, Feng YF (2014) An experimental study of crack coalescence behaviour in rock-like materials containing multiple flaws under uniaxial compression. *Rock Mech Rock Eng* 47(6):1961–1986
- Zhu C, Arson C (2015) A model of damage and healing coupling halite thermo-mechanical behavior to microstructure evolution. *Geotech Geol Eng* 33(2):389–410